RESEARCH ARTICLE

Low-Carbon Economic Dispatch of Integrated Electricity-Gas Energy System Considering Carbon Capture, Utilization and Storage

XINGHUA LIU[1], (Senior Member, IEEE), **XIANG LI**[1], (Student Member, IEEE),
JIAQIANG TIAN[2], **GUOQING YANG**[1], **HUIBAO WU**[3], **RONG HA**[4],
AND PENG WANG[5], (Fellow, IEEE)

[1]School of Electrical Engineering, Xi'an University of Technology, Xi'an 710048, China
[2]School of Electrical Engineering and Automation, Anhui University, Hefei 230039, China
[3]State Grid Xi'an Electric Power Supply Company, Xi'an 710000, China
[4]Xi'an Jinze Electric Technology Company Ltd., Xi'an 710100, China
[5]School of Electrical and Electronic Engineering, Nanyang Technological University, Singapore 639798

Corresponding author: Xinghua Liu (liuxh@xaut.edu.cn)

ABSTRACT With the rapid development of modern industry, while improving people's living standards, the over-exploitation of coal, oil and natural gas has led to a shortage of fossil energy, global warming and an increasingly serious deterioration of the ecological environment. To mitigate the greenhouse effect caused by excessive carbon emissions, the vigorous development of integrated electricity-gas system (IEGS) dominated by clean energy is the future trend of sustainable development of energy systems. In this paper, a bi-level optimal scheduling model is proposed for an IEGS considering carbon capture, utilization and storage (CCUS), and the ladder carbon trading mechanism is introduced to convert carbon emissions into economic benefits. The upper model is an optimal distribution model of natural gas network, and the lower model is a day-ahead economic dispatch model of power system. Based on the Karush-Kuhn-Tucher (KKT) condition and strong duality theory of the lower model, the bi-level model is transformed into a mixed integer linear programming (MILP), which is solved by calling CPLEX through the Yalmip toolbox of the Matlab platform. Finally, the reasonableness and validity of the model are verified by three arithmetic simulations. The results show that the proposed bi-level model for low-carbon economic dispatch of IEGS considering CCUS can effectively reduce the operating costs and carbon emissions of the system.

INDEX TERMS Low-carbon electricity, integrated electricity-gas system (IEGS), economic dispatch, carbon capture, utilization and storage (CCUS), mixed integer linear programming (MILP).

NOMENCLATURE

P_i	Active power of node i.
Q_i	Reactive power of node i.
$\dot{U}_i$	Node voltage of node i.
$\dot{U}_j$	Node voltage of node j.
$\dot{Y}_{ij}$	Conductivity of the power branch ij.
$U_{i,\max}$	Maximum values of voltage at node i.
$U_{i,\min}$	Minimum values of voltage at node i.
$P_{i,\max}$	Maximum values of active power of node i.
$P_{i,\min}$	Minimum values of active power of node i.
$Q_{i,\max}$	Maximum values of reactive power for node i.
$Q_{i,\min}$	Minimum values of reactive power for node i.
δ_i	Phase angle of node i.
δ_j	Phase angle of node j.

The associate editor coordinating the review of this manuscript and approving it for publication was Ali Raza.

L_{ij}	Value of current flowing through line ij.	$Q_{R,sto}$	Rated capacity of carbon storage device.
L_{ij}^{max}	Current transmission limit of branch ij.	c_j	Natural gas price.
$F_{mn}(t)$	Flow of natural gas through natural gas pipeline mn at time t.	c_i	Thermal power unit operating cost factor.
S_{mn}	Direction parameter, indicating the direction of natural gas flow in the pipeline.	c_{P2G}	P2G operating cost factor.
		c_g	Gas turbine operating cost factor.
σ_{mn}	Pipe parameters.	c_w	Wind curtailment cost factor.
θ_m	Air pressure of node m.	ω_t	Wind power utilization.
θ_n	Air pressure of node n.	$P_w(t)$	Wind turbine output power.
$S_j(t)$	Natural gas supply from the gas source station at time t.	c_E	Time-of-use electricity price.
S_j^{min}	Lower gas supply limits at gas supply stations.	λ_c	Carbon storage cost factor.
		G_i^{max}	Upper limits of the output power of the generator set.
S_j^{max}	Upper gas supply limits at gas supply stations.	G_i^{min}	Lower limits of the output power of the generator set.
$H_{c,mn}$	Compressor operation energy consumption.	P_w^{max}	Maximum value of wind power at time t.
τ_{mn}	Equivalent flow of energy consumed by compressor.	$Q_{R,sto}$	Rated capacity of carbon storage device.
v_1, v_2, v_3	Energy conversion efficiency constant.	U	Decision variable.
$\theta_{m,max}$	Upper limits of node m pressure.	*Abbreviations*	
$\theta_{m,min}$	Lower limits of node m pressure.	CCUS:	Carbon capture, utilization and storage.
$S_{P2G}(t)$	Amount of synthetic natural gas produced by the P2G device at time t.	IEGS:	Integrated electricity-gas system.
$S_g(t)$	Amount of natural gas consumed by gas turbine operation at time t.	KKT:	Karush-Kuhn-Tucher.
		MILP:	Mixed integer linear programming.
S_{load}	Gas load.	LSEs:	Load serving entities.
$P_{CCPP}(t)$	Energy consumed by the carbon capture device at time t.	SNG	Synthetic natural gas.
		CCPP:	Carbon capture power plant.
$P_r^{CCPP}(t)$	Operating energy consumption of carbon capture device at time t.	IGCC	Integrated gasification combined cycle.
P_b^{CCPP}	Basic energy consumption.		
μ	Energy consumed to capture per CO_2.		
η_t	Carbon capture rate.		
δ_t	Carbon emissions intensity of generator set.		
$G_i(t)$	Output power of the generator set at time t.		
$Q_{CCPP}(t)$	CCPP actual carbon emissions.		
$P_{P2G}(t)$	Power consumed by the P2G device at time t.		
η_{P2G}	P2G efficiency.		
$P_{R,P2G}$	Rated power of P2G device.		
LHV	Natural gas calorific value.		
$P_g(t)$	Output power of the gas turbine.		
$P_{R,GT}$	Rated power of gas turbine.		
F_c	Carbon trading cost.		
E_{IES}	Total carbon emissions of the system in a dispatch period.		
c	Carbon emissions trading price.		
s	Carbon trading price growth rate for each tier.		
x	Carbon emission range length.		
Q_t	Carbon emission quota.		
$Q_{sto}(t)$	Carbon storage at time t.		
λ_c	Carbon storage cost factor.		

I. INTRODUCTION

In recent years, with the rapid development of social productivity, the energy utilization pattern mainly in the form of fossil fuel combustion has caused serious environmental pollution [1]. A large amount of CO_2 emitted by combustion is the main cause of the greenhouse effect. As a major energy-consuming industry, the power sector accounts for 42% of the world's total CO_2 emissions [2]. Therefore, the vigorous development of low-carbon electricity is of great significance to the reduction of carbon emissions and the sustainable development of electricity [3]. With the development of gas turbine power generation technology, natural gas has become one of the important energy sources for power generation due to its wide reserves, low cost and high safety [4]. The future energy system is the product of a highly coupled electricity and natural gas network.

Integrated electricity-gas system (IEGS) is a kind of integrated energy system, which can consolidate primary energy sources such as coal, oil, natural gas and renewable energy sources such as wind and photovoltaic in a certain region by using advanced physical information technology and innovative management mode [5]. It realizes coordinated planning, optimized operation, collaborative management, interactive response and complementary mutual benefit between multiple heterogeneous energy subsystems [6]. The IEGS contains two energy networks, the electric network and the natural gas network. The energy flow between the two systems is bi-directional through gas turbines and power-to-gas (P2G)

units. The P2G device converts excess wind energy into synthetic natural gas (SNG) through an electrolytic water reaction and a methane catalytic reaction, providing a different solution for the consumption of clean energy [7]. CO_2 from primary energy combustion can be used as feedstock for SNG production in the P2G device, which can effectively reduce system carbon emissions.

At present, most of the research on IEGS has focused on economic scheduling [8]. Paper [9] considers the effect of power-to-gas equipment on wind power consumption in the electricity-gas integrated energy system to improve the system economy. In [10], an operation optimization strategy of the integrated energy system of the park based on the primary-secondary game of the source-load dual side is proposed, which takes into account the interests of different subjects in the process of operation optimization and improves the economic benefits of each subject in the system. The above paper investigates the overall dispatch of the system but does not consider the economic dispatch under market intervention. In [11], to address the complexity of bidding decisions in the electricity market, a new strategic bidding model for a load serving entities (LSEs) is proposed in which the primary objective is to maximize the LSE's profit by providing optimal load serving entities considering high wind power penetration. The paper [12] proposes a model of an integrated electricity-gas-heat energy system under the participation of multiple markets by considering the market benefits and operating costs, and the integrated benefits can be maximized through system coordination and cooperation. The above paper considers the economic benefits in a variety of markets but ignores the issue of environmental pollution. Paper [13] proposes a joint economic operation model for an integrated electricity-gas interconnection energy system, and introduces a carbon trading mechanism. The two low-carbon economic operation states under the model of an integrated electricity-gas interconnection energy system and a pure thermal power generation system considering the carbon trading mechanism are compared. Paper [14] proposes an opportunity constrained and reliability planning optimization model that minimizes the capital and operating costs of the electricity and natural gas transmission system under probabilistic constraints to achieve the desired level of confidence in supply.

Carbon capture, utilization and storage (CCUS) technology is considered to be one of the effective measures that can reduce carbon emissions [15]. The CO_2 captured and stored by CCUS can be used as raw material for SNG production from P2G in IEGS [16]. Therefore, the CCUS system can significantly reduce the carbon emissions of IEGS. Existing carbon capture technologies are divided into three categories: pre-combustion capture, oxygen-enriched combustion capture and post-combustion capture.

A. PRE-COMBUSTION CAPTURE
Pre-combustion capture is the removal of CO_2 from coal or fossil fuels before the actual combustion process begins,
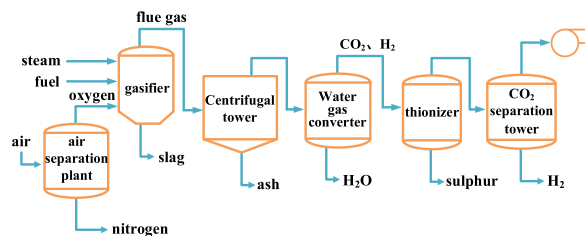

FIGURE 1. Pre-combustion capture flow chart.

in which an air separation unit delivers the separated oxygen to the gas generator. The CO_2 is separated and stored after the mixture is desulfurized, and the remaining high concentration of H_2 is used as fuel. However, the application scope of pre-combustion capture technology is limited to integrated gasification combined cycle (IGCC) system, and it has the disadvantages of high upfront investment cost and low reliability. The specific process is shown in Fig. 1.

B. OXYGEN-ENRICHED COMBUSTION CAPTURE
In oxyfuel combustion carbon capture technology, a large percentage of nitrogen is initially removed from the air in the air separation unit by oxygen production technology, and a mixture of highly concentrated oxygen and a portion of the extracted flue gas is used directly in place of air. The fuel is burned under this gas mixture, so the flue gas produced after combustion consists mainly of high concentrations of CO_2 and water vapor, which can be directly processed for carbon sequestration. The challenges of oxygen-enriched combustion capture technology are the high cost of oxygen production and the high energy consumption ratio. The specific process is shown in Fig. 2.
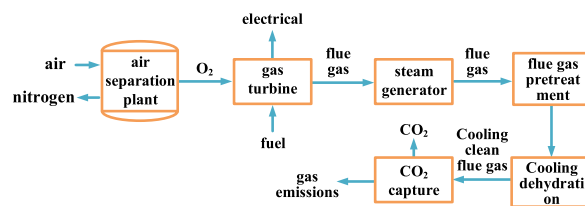

FIGURE 2. Oxygen-enriched combustion capture flow chart.

C. POST-COMBUSTION CAPTURE
Post-combustion capture is a technology that separates CO_2 from a flue gas pipe filled with a mixture of gases after the fossil fuel has been fully combusted. The main capture methods are chemical absorption, adsorption, physical absorption and membrane separation. Post-combustion capture technology is simple in principle and has a wide range of applications. It is considered to be the most feasible capture method at present. The specific process is shown in Fig. 3.

There have been more studies considering CCUS in IES. In [17], the operation mechanism and peaking performance of carbon capture power plants were investigated in depth with the basic principles of carbon capture technology, and the problem of the significant decrease in carbon capture level
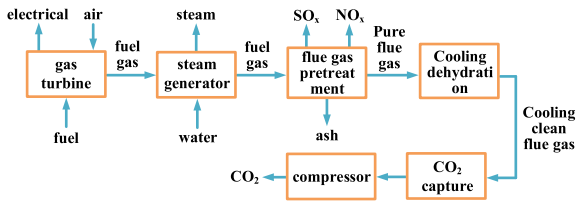
FIGURE 3. Post-combustion capture flow chart.

occurs during peaking, so peak shaving measures need to be considered. Paper [18] introduces an independent carbon capture system on the basis of thermal power units to achieve the purpose of improving the wind power consumption rate and reducing carbon emissions, but it does not fully utilize the captured CO_2. While all of the above paper considers methods to reduce carbon emissions, it does not investigate the economic value of CO_2 in depth. Based on the CCUS-P2G coordinated operation framework, Paper [19] proposes a low-carbon economic dispatch model for the IEGS with combined operation of CCUS and P2G. The simulation results show that the proposed model can enhance the system's renewable energy consumption and reduce costs and carbon emissions.

The carbon trading mechanism is a market mechanism to trade carbon emission credits as a commodity, and companies can purchase or sell carbon emission credits according to their demands. The ladder carbon trading mechanism divides carbon emissions into multiple bands on the basis of the traditional carbon trading mechanism, and each band corresponds to a different unit carbon trading price, which can more effectively drive the enthusiasm of enterprises to save energy and reduce emissions. In [20], a low carbon economic dispatch model considering scenario probability including wind power is proposed. By introducing the traditional carbon trading mechanism, it is proved that it can effectively reduce carbon emissions and increase the output of low-carbon units. Paper [21] proposes an optimal dispatching model of electricity-gas integrated energy system with the introduction of carbon trading mechanism to analyze the impact of carbon trading formulation on the economy and carbon emission, which is a guideline for low-carbon economic dispatching of the integrated energy system. However, the model does not consider the case of the ladder carbon trading mechanism.

Motivated by the above observations, a bi-level optimal scheduling model of IEGS considering carbon capture, utilization and storage is proposed. The upper model is the optimal distribution model for the natural gas networks, and the lower model is the day-ahead economic dispatch model for power system. The introduction of a ladder carbon trading mechanism has effectively reduced system carbon emissions and carbon trading costs. The detailed contributions of this article are as follows.

1) The proposed low carbon scheduling model considering CCUS has a positive impact on the IEGS in terms of carbon emission reduction and economical operation. Besides, CCUS can participate in the operation of the system as a load, providing more solutions for clean energy consumption and improving the operational flexibility of IEGS.

2) The optimal scheduling problems of power system and natural gas system are modeled hierarchically in this paper. In comparison with the single-level model that directly sums the objective functions of two systems [22], the bi-level model can obviously reduce the operating cost of IEGS.

3) Compared with the traditional carbon trading mechanism [23], the ladder carbon trading mechanism in this paper has a more reasonable intensity of carbon emission rewards and penalties. It can effectively drive the enthusiasm of enterprises to save energy and reduce emissions.

The arrangement of paper is organized as follows. In Section II, CCUS and ladder carbon trading mechanism models are proposed. In Section III, the modeling of the bi-level model is provided. In Section IV, the solution process of the bi-level model is given. In Section V, three comparative experiments are presented to prove the rationality of the proposed model. Finally, some concluding remarks are given in Section VI.

II. SYSTEM DESCRIPTION AND MODEL
A. POWER NETWORK MODEL
Power system tide calculation is a method to study the steady-state operation of a power system, which determines the operating state of the entire power system components based on the given operating conditions and system wiring. In both the design of power system planning and the study of existing power system operation methods, it is necessary to use tidal wave calculation to quantitatively analyze the rationality, reliability and economy of the operation methods. As the same as the traditional power system tide modeling, the power system in IEGS is calculated using the Newton-Raphson method (N-L method), one of the common algorithms for power system tide calculation, which has the advantages of good convergence and low number of iterations.

1) Power balance constraint:

$$P_i + jQ_i - \dot{U}_i \sum_{j=1}^{n} \dot{Y}_{ij} \dot{U}_j = 0 \qquad (1)$$

where P_i is active power of node i. Q_i is reactive power of node i. $\dot{U}_i$ and $\dot{U}_j$ are node voltage of node i and node j respectively. $\dot{Y}_{ij}$ is conductivity of the power branch ij.

2) Node voltage constraint:

$$U_{i,\min} \leq U_i \leq U_{i,\max} \qquad (2)$$

where $U_{i,\max}$ and $U_{i,\min}$ are maximum and minimum values of voltage at node i.

3) Power upper and lower limits constraint:

$$P_{i,\min} \leq P_i \leq P_{i,\max} \qquad (3)$$

$$Q_{i,\min} \leq Q_i \leq Q_{i,\max} \qquad (4)$$

where $P_{i,\min}$ and $P_{i,\max}$ are minimum and maximum values of active power of node i. $Q_{i,\min}$ and $Q_{i,\max}$ minimum and maximum values of reactive power for node i.

4) Phase difference constraint:

$$\left|\delta_i - \delta_j\right| < \left|\delta_i - \delta_j\right|_{\max} \tag{5}$$

where δ_i and δ_j are phase angle of node i and node j.

5) Line transmission constraint:

$$0 \leq L_{ij} \leq L_{ij}^{\max} \tag{6}$$

where L_{ij} is value of current flowing through line ij. $L_{ij}^{\max}$ is current transmission limit of branch ij.

B. NATURAL GAS NETWORK MODEL
Natural gas is a key component of the energy transition and it will play a critical role in the future energy grid. Compared to other fossil fuels, natural gas power generation is characterized by a lower environmental impact, high conversion efficiency, low capital investment costs, short construction time and high operational flexibility. The main components of a natural gas network are gas source stations, compressors, transmission pipelines and gas loads.

1) NATURAL GAS FLOW EQUATION
Natural gas pipeline flow is influenced by pipeline length, width, operating temperature and node air pressure. For the natural gas pipeline mn, similar to the node voltage of the electrical network, the node air pressure at nodes m and n of the natural gas pipeline network affects the flow of natural gas, i.e., the flow flows from the node with high air pressure to the node with low air pressure. The pipeline flow rate of the natural gas system can be approximated by the Weymouth equation, which is expressed as:

$$F_{mn}(t) = S_{mn} \cdot \sigma_{mn}\sqrt{\left|\theta_m^2 - \theta_n^2\right|} \tag{7}$$

$$S_{mn} = \begin{cases} 1, & \theta_m \geq \theta_n \\ -1, & \theta_m < \theta \end{cases} \tag{8}$$

where $F_{mn}(t)$ is flow of natural gas through natural gas pipeline mn at time t. S_{mn} is direction parameter, indicating the direction of natural gas flow in the pipeline, when the pressure at node m is higher than node n is taken as 1, and vice versa is taken as -1. σ_{mn} indicates pipe parameters related to pipe length, temperature, diameter, etc. θ_m and θ_n are air pressure of node m and node n.

2) GAS SOURCE STATION CONSTRAINT
In actual operation, natural gas cannot be supplied indefinitely, so the supply of natural gas from the gas source station needs to be bounded by upper and lower limits, which can be expressed as:

$$S_j^{\min} \leq S_j(t) \leq S_j^{\max} \tag{9}$$

where $S_j(t)$ is natural gas supply from the gas source station at time t. $S_j^{\min}$ and $S_j^{\max}$ are lower and upper gas supply limits at gas supply stations.

3) PRESSURE STATION MODEL
In the long-distance transportation of natural gas, in order to offset the gradual decrease of the transportation pressure caused by the flow resistance, and ensure the transportation volume and the pressure at the destination, the pressure station needs to be set up on the way.

$$H_{c,mn} = Z \cdot F_{mn}\left[\left(\frac{\theta_m}{\theta_n}\right)^K - 1\right] \tag{10}$$

$$\tau_{mn} = v_1 H_{c,mn}^2 + v_2 H_{c,mn} + v_3 \tag{11}$$

where $H_{c,mn}$ is compressor operation energy consumption. Z and K are constants. τ_{mn} is equivalent flow of energy consumed by compressor. v_1, v_2, v_3 are energy conversion efficiency constant.

4) NODE PRESSURE CONSTRAINT

$$\theta_{m,\min} \leq \theta_m \leq \theta_{m,\max} \tag{12}$$

where $\theta_{m,\min}$ and $\theta_{m,\max}$ are lower and upper limits of node m pressure.

5) NATURAL GAS FLOW BALANCE CONSTRAINT

$$\sum_{j=1}^{N_j} S_j(t) + \sum_{p=1}^{N_p} S_{P2G}(t) - \sum_{m=1}^{N_m} S_g(t) - S_{load} = 0 \tag{13}$$

where $S_{P2G}(t)$ is the amount of synthetic natural gas produced by the P2G device at time t. $S_g(t)$ the amount of natural gas consumed by gas turbine operation at time t. S_{load} is gas load.

C. CCPP OPERATION CHARACTERISTICS
Retrofitting conventional thermal power plants with carbon capture devices to form carbon capture power plants (CCPP). The flue gas from the combustion of thermal power units is captured by a carbon capture system and then passes through a series of processes to reach the CO_2 regeneration tower. A portion of this is used to produce synthetic natural gas for P2G and the other portion flows to CO_2 compressor for storage. After the decarbonisation process, the mixed solution flows to the CO_2 absorption tower for subsequent use [24].

The energy consumption of carbon capture devices includes operating energy consumption and primary energy consumption. The basic energy consumption is fixed, independent of the operation state of the carbon capture device. Operating energy consumption mainly refers to the energy consumption generated by the carbon capture system in capturing CO_2 [25]. Operating energy consumption is related to the operating condition of the carbon capture system. The carbon capture device can change the net output power by adjusting the operating energy consumption of the carbon capture system, thus improving the wind absorption capacity of the system.

$$P_{CCPP}(t) = P_r^{CCPP}(t) + P_b^{CCPP} \tag{14}$$

$$P_r^{CCPP}(t) = \mu \cdot \eta_t \cdot \delta_t \cdot \sum_{g=1}^{N_g} G_i(t) \qquad (15)$$

$$Q_{CCPP}(t) = (1 - \eta_t) \cdot \delta_t \cdot \sum_{g=1}^{N_g} G_i(t) \qquad (16)$$

$$\underline{\eta} \leq \eta_t \leq \overline{\eta} \qquad (17)$$

where $P_{CCPP}(t)$ is the energy consumed by the carbon capture device at time t. $P_r^{CCPP}(t)$ is operating energy consumption of carbon capture device at time t. P_b^{CCPP} is basic energy consumption. μ is the energy consumed to capture per CO_2. η_t is the carbon capture rate. δ_t is carbon emissions intensity of generator set. $G_i(t)$ is the output power of the generator set at time t. $Q_{CCPP}(t)$ is CCPP actual carbon emissions.

D. POWER-TO-GAS MODEL

P2G technology mainly includes two types: power-to-hydrogen and power-to-methane [26]. The flow of P2G implementation is shown in Fig. 4. P2G technology facilitates large-scale storage of natural gas, provides natural gas directly to the gas load, and converts natural gas to electricity via gas turbines when required by the electric load. It not only promotes CO_2 reduction by reducing the output of thermal power units but also reduces the dependence on the natural gas network at the gas source. The relationship that P2G consumes power to generate SNG is formulated as (18). The upper and lower limits of energy consumption and conversion efficiency of P2G device in period t are shown in (19)-(20).

$$S_{P2G}(t) = \frac{P_{P2G}(t) \cdot \eta_{P2G}}{LHV} \qquad (18)$$

$$\eta_{P2G}^{min} \leq \eta_{P2G} \leq \eta_{P2G}^{max} \qquad (19)$$

$$0 \leq P_{P2G}(t) \leq P_{R,P2G} \qquad (20)$$

where $S_{P2G}(t)$ is the amount of natural gas produced by the P2G device at time t. $P_{P2G}(t)$ is the power consumed by the P2G device at time t. η_{P2G} is P2G efficiency. $P_{R,P2G}$ is rated power of P2G device. LHV is the natural gas calorific value.

Currently, the energy conversion efficiency of the complete process of electricity to natural gas conversion can reach 45%-60%. In Germany, where conversion technology is more developed, P2G has been used to improve the utilization of renewable energy and achieve CO_2 emission reduction targets, and a commercial P2G demonstration project has been built [27].

E. GAS TURBINE MODEL

For the power system, the gas turbine is the energy supply side resource, while it is a load in the natural gas system [28]. The power generation of the gas power plants is proportional to the natural gas consumption, and the conversion relationship can be approximately formulated as (21)-(22).

$$P_g(t) = S_g(t) \cdot LHV \cdot \eta_g \qquad (21)$$
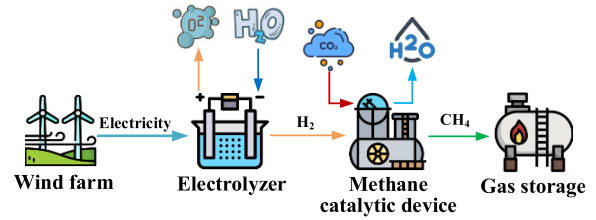
$$0 \leq P_g(t) \leq P_{R,GT} \qquad (22)$$
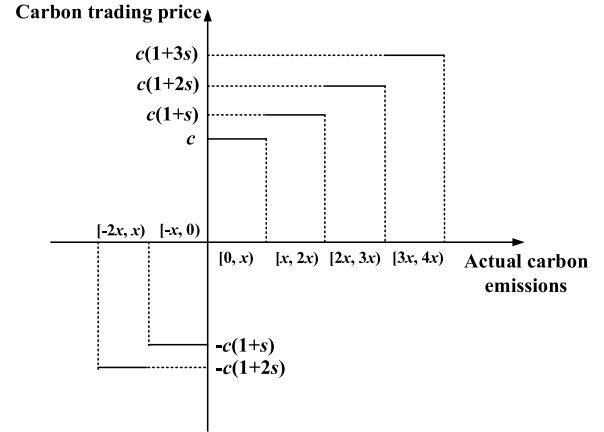

FIGURE 4. P2G flow chart.

FIGURE 5. Ladder carbon trading mechanism.

where $P_g(t)$ is the output power of the gas turbine. $S_g(t)$ is the natural gas consumed during the operation of the gas turbine. $P_{R,GT}$ is rated power of gas turbine.

F. LADDER CARBON TRADING MECHANISM MODEL

The carbon trading mechanism treats carbon emissions as a freely tradable commodity. The regulator allocates carbon credits to each source to control the total amount of carbon emissions, carbon credits refer to the total amount of CO_2 that enterprises are allowed to emit by the regulator for a limited period of time, and if the actual carbon emissions of the source are higher than the allocated amount, it is required to purchase the excess credits in the carbon trading market. Conversely, when the actual carbon emissions of a source are less than the allocated amount, it can sell the remaining credits in the carbon trading market. Thus, the carbon trading mechanism both punishes high carbon emitters economically and rewards the energy-saving sector, which makes carbon emissions have a great economic value [29]. The ladder carbon trading mechanism refers to the division of carbon emissions into multiple bands, with the higher carbon emissions corresponding to higher carbon trading prices [30]. In this transaction cost model, the relationship between carbon trading volume and price is shown in Fig. 5. In the figure, x is an interval length, when carbon emissions are within the interval from ($0 \sim x$), the carbon trading price is c; when carbon emissions are within the interval from ($x \sim 2x$), the carbon trading price for the part within the x interval is still c, and the carbon trading price for the part beyond x is $c(1 + s)$, and so on.

In summary, the system carbon transaction cost can be formulated as (23).

$$
F_C = \begin{cases}
\ldots \\
-c(1+s)x - c(1+2s)(Q_t - x - E_{IES}) \\
\quad , Q_t - 2x < E_{IES} \leq Q_t - x \\
-c(1+s)(Q_t - x - E_{IES}) \\
\quad , Q_t - x < E_{IES} \leq Q \\
c(E_{IES} - Q_t) \\
\quad , Q_t < E_{IES} \leq Q_t + x \\
cx + c(1+s)(E_{IES} - Q_t - x) \\
\quad , Q_t + x < E_{IES} \leq Q_t + 2x \\
c(2+s)x + c(1+2s)(E_{IES} - Q_t - 2x) \\
\quad , Q_t + 2x < E_{IES} \leq Q_t + 3x \\
c(3+3s)x + c(1+3s)(E_{IES} - Q_t - 3x) \\
\quad , Q_t + 3x < E_{IES} \leq Q_t + 4x \\
\ldots
\end{cases}
\tag{23}
$$

where F_c is the carbon trading cost. E_{IES} is the total carbon emissions of the system in a dispatch period. c is carbon emissions trading price. s is the carbon trading price growth rate for each tier. x is the carbon emission range length. Q_t carbon emission quota.

G. CARBON STORAGE MECHANISM MODEL
Carbon storage is the safe storage of captured carbon to avoid emission into the atmosphere. At present, the research direction of carbon storage is mostly deep-sea storage and geological saline aquifer storage [31]. The principle is to use the rich calcium and magnesium ions in seawater and saline aquifer to react with CO_2 to generate solid materials for storage.

$$
F_{sto}(t) = \lambda_c \cdot Q_{sto}(t)
\tag{24}
$$

$$
0 \leq \sum_{t=1}^{T} Q_{sto}(t) \leq Q_{R,sto}
\tag{25}
$$

where $Q_{sto}(t)$ is carbon storage at time t. λ_c is carbon storage cost factor. $Q_{R,sto}$ is rated capacity of carbon storage device.

III. BI-LEVEL DISPATCH MODEL
The IEGS consists of wind farms, CCPP, gas source, P2G device, gas turbine, carbon storage device, electricity load and natural gas load. The diagram of the IEGS is shown in Fig. 6. P2G and gas sources can participate in the scheduling of IEGS as electricity and gas load. The CO_2 required for the production of synthetic natural gas can be taken away from the CO_2 captured by the carbon capture unit. This reduces carbon emissions and environmental pollution. In addition, when the wind energy is in surplus, P2G can convert the unconsumable wind power to natural gas. The carbon capture device changes the net power output by regulating the energy consumption of carbon capture. The coordinated operation of both greatly improves the wind power consumption capacity of the system.
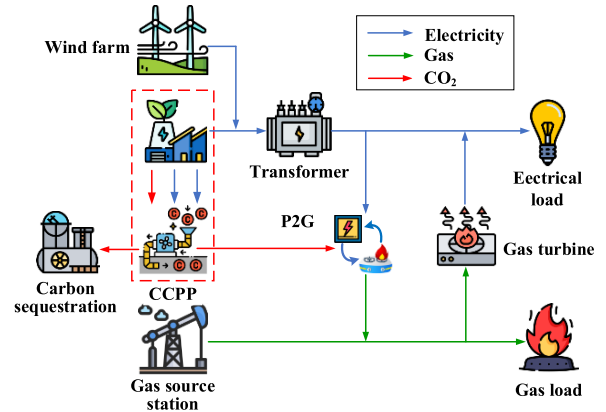

FIGURE 6. Integrated electricity-gas energy system structure diagram.

A. UPPER NATURAL GAS SYSTEM MODEL
In the natural gas system, gas resources are distributed to consumers through the gas transmission network from the gas source. In the natural gas network, it is assumed that each gas source sells gas at different prices and its gas sales cost is proportional to the gas sales volume. The objective function of the optimal scheduling of the upper-level natural gas system is to minimize the total cost of natural gas system operation, and the constraint condition is the natural gas network constraint. Therefore, the upper-level natural gas system dispatching model can be expressed as (26)-(28).

$$
F_g = \min \sum_{t=1}^{T} \sum_{j=1}^{N_j} (c_j \cdot S_j(t))
$$
$$
s.t. \quad (7)-(13), (18)-(20)
\tag{26}
$$

$$
\sum_{j=1}^{N_j} S_j(t) + \sum_{p=1}^{N_p} S_{P2G}(t) - \sum_{m=1}^{N_m} S_g(t) - S_{load} = 0
\tag{27}
$$

$$
S_{j,\min} \leq S_j(t) \leq S_{j,\max}
\tag{28}
$$

where c_j is the natural gas price. $S_j(t)$ is gas purchase volume. $S_g(t)$ is gas consumption of gas turbine. $S_{j,\max}$, $S_{j,\min}$ are the upper and lower limits of the gas supply volume of the gas source station.

B. LOWER POWER SYSTEM MODEL
The objective of the day-ahead economic dispatch problem of the lower power system is to minimize the operating cost. Including thermal power generation costs, P2G and gas turbine operating costs, wind curtailment costs, carbon capture device operating costs, carbon storage costs, and carbon trading costs.

$$
F_e = \min \sum_{t=1}^{T} \left(\sum_{g=1}^{N_g} c_i \cdot G_i(t) + \sum_{w=1}^{N_w} c_w(1-\omega_t)P_w(t) \right.
$$
$$
+ \sum_{m=1}^{N_m} c_g \cdot P_g(t) + \sum_{p=1}^{N_p} c_{P2G} \cdot P_{P2G}(t)
$$
$$
\left. + c_E \cdot P_{CCPP}(t) + \lambda_c \cdot Q_{sto}(t) \right)
\tag{29}
$$

$$s.t. \quad \sum_{g=1}^{N_g} G_i(t) + \sum_{w=1}^{N_w} \omega_t \cdot P_w(t) + \sum_{m=1}^{N_m} P_g(t)$$

$$- \sum_{p=1}^{N_p} P_{P2G}(t) - P_{CCPP}(t) - P_{load} = 0 : \lambda_t$$

(30)

$$G_i^{\min} \le G_i(t) \le G_i^{\max} : \mu^{\min}, \mu^{\max} \quad (31)$$

$$0 \le P_w(t) \le P_w^{\max} : \phi^{\min}, \phi^{\max} \quad (32)$$

$$0 \le \sum_{t=1}^{T} Q_{sto}(t) \le Q_{R,sto} : \gamma^{\min}, \gamma^{\max} \quad (33)$$

$$0 \le P_g(t) \le P_{R,GT} : \eta^{\min}, \eta^{\max} \quad (34)$$

$$0 \le P_{P2G}(t) \le P_{R,P2G} : \pi^{\min}, \pi^{\max} \quad (35)$$

where c_i is thermal power unit operating cost factor. $G_i(t)$ is the output power of the generator set at time t. c_{P2G} is P2G operating cost factor. $P_{P2G}(t)$ is the power consumed by the P2G device at time t. c_g is gas turbine operating cost factor. $P_g(t)$ is the output power of the gas turbine. c_w is wind curtailment cost factor. ω_t is wind power utilization. $P_w(t)$ is wind turbine output power. c_E is time-of-use electricity price. λ_c is carbon storage cost factor. $Q_{sto}(t)$ is CO_2 sequestered at time t. $G_i^{\max}, G_i^{\min}$ are the upper and lower limits of the output power of the generator set. $P_w^{\max}$ is the maximum value of wind power at time t. $Q_{R,sto}$ is rated capacity of carbon storage device. $P_{R,GT}$ is rated power of gas turbine. $P_{R,P2G}$ is rated power of P2G. λ_t, $\mu^{\min}$, $\mu^{\max}$, $\phi^{\min}$, $\phi^{\max}$, $\gamma^{\min}$, $\gamma^{\max}$, $\eta^{\min}$, $\eta^{\max}$, $\pi^{\min}$, $\pi^{\max}$ are the Lagrange multipliers corresponding to the objective function and constraints.

IV. BI-LEVEL MODEL MATHEMATICAL SOLUTION

The bi-level model established in this paper considers the economics of the operation of the two systems separately. Given that the lower-level model is a linear programming problem. By reformulating the lower-level problem as its KKT optimality condition, the dual objective function of the lower-level model is then derived based on strong dual theory and added to the upper-level model. Thus, the bi-level model is transformed into a single-level model. Finally, eliminating the nonlinear terms in it is considered to transform the model into a more easily solvable MILP problem. The process of the bi-level model converted to a single-level model is as follows:

$$L = \sum_{t=1}^{T} (\sum_{g=1}^{N_g} c_i \cdot G_i(t) + \sum_{p=1}^{N_p} c_{P2G} \cdot P_{P2G}(t) + \sum_{m=1}^{N_m} c_g \cdot P_g(t)$$

$$+ \sum_{w=1}^{N_w} c_w(1-\omega_t)P_w(t) + c_E \cdot P_{CCPP}(t) + \lambda_c \cdot Q_{sto}(t))$$

$$+ \lambda_t \cdot (\sum_{g=1}^{N_g} G_i(t) + \sum_{w=1}^{N_w} \omega_t \cdot P_w(t) + \sum_{m=1}^{N_m} P_g(t)$$

$$- \sum_{p=1}^{N_p} P_{P2G}(t)$$

$$- P_{CCPP}(t) - P_{load}(t)) + \sum_{g=1}^{N_g} \mu^{\min}(G_i^{\min} - G_i(t))$$

$$\sum_{g=1}^{N_g} \mu^{\max}(G_i(t) - G_i^{\max}) + \sum_{w=1}^{N_w} \phi^{\min} \cdot (0 - P_w(t))$$

$$\sum_{w=1}^{N_w} \phi^{\max} \cdot (P_w(t) - P_w^{\max}) + \sum_{p=1}^{N_p} \pi^{\min} \cdot (0 - P_{P2G}(t))$$

$$\sum_{p=1}^{N_p} \pi^{\max} \cdot (P_{P2G}(t) - P_{R,P2G}) + \sum_{m=1}^{N_m} \eta^{\min} \cdot (0 - P_g(t))$$

$$\sum_{m=1}^{N_m} \eta^{\max} \cdot (P_g(t) - P_{R,GT}) + \gamma^{\min} \cdot (0 - Q_{sto}(t))$$

$$\gamma^{\max} \cdot (Q_{sto}(t) - Q_{R,sto}) \quad (36)$$

Firstly, the Lagrangian function of the lower model is constructed, as shown in (36). The complementary relaxation condition of the lower model can be written as (37)-(46).

$$0 \le \mu^{\max} \perp (G_i^{\max} - G_i(t)) \ge 0 \quad (37)$$

$$0 \le \mu^{\min} \perp (G_i(t) - G_i^{\min}) \ge 0 \quad (38)$$

$$0 \le \pi^{\max} \perp (P_{R,P2G} - P_{P2G}(t)) \ge 0 \quad (39)$$

$$0 \le \pi^{\min} \perp P_{P2G}(t) \ge 0 \quad (40)$$

$$0 \le \phi^{\max} \perp (P_w^{\max} - P_w(t)) \ge 0 \quad (41)$$

$$0 \le \phi^{\min} \perp P_w(t) \ge 0 \quad (42)$$

$$0 \le \eta^{\max} \perp (P_{R,GT} - P_g(t)) \ge 0 \quad (43)$$

$$0 \le \eta^{\min} \perp P_g(t) \ge 0 \quad (44)$$

$$0 \le \gamma^{\min} \perp Q_{sto}(t) \ge 0 \quad (45)$$

$$0 \le \gamma^{\max} \perp (Q_{R,sto} - Q_{sto}(t)) \ge 0 \quad (46)$$

The complementarity constraints (37)-(46) are nonlinear. The linearization for them is presented below. In accordance with the big-M method. By introducing auxiliary decision variable U, the complementary relaxation condition can be linearized.

$$0 \le \mu^{\max} \le M_\mu^{\max} \cdot U_\mu^{\max} \quad (47)$$

$$0 \le G_i^{\max} - G_i(t) \le M_\mu^{\max} \cdot (1 - U_\mu^{\max}) \quad (48)$$

$$0 \le \mu^{\min} \le M_\mu^{\min} \cdot U_\mu^{\min} \quad (49)$$

$$0 \le G_i(t) - G_i^{\min} \le M_\mu^{\min} \cdot (1 - U_\mu^{\min}) \quad (50)$$

$$0 \le \pi^{\max} \le M_\pi^{\max} \cdot U_\pi^{\max} \quad (51)$$

$$0 \le P_{R,P2G} - P_{P2G}(t) \le M_\pi^{\max} \cdot (1 - U_\pi^{\max}) \quad (52)$$

$$0 \le \pi^{\min} \le M_\pi^{\min} \cdot U_\pi^{\min} \quad (53)$$

$$0 \le P_{P2G}(t) \le M_\pi^{\min} \cdot (1 - U_\pi^{\min}) \quad (54)$$

$$0 \le \phi^{\max} \le M_\phi^{\max} \cdot U_\phi^{\max} \quad (55)$$

$$0 \le P_w^{\max} - P_w(t) \le M_\phi^{\max} \cdot (1 - U_\phi^{\max}) \quad (56)$$

$$0 \le \phi^{\min} \le M_\phi^{\min} \cdot U_\phi^{\min} \quad (57)$$

$$0 \le P_w(t) \le M_\phi^{\min} \cdot (1 - U_\phi^{\min}) \quad (58)$$

$$0 \le \eta^{\max} \le M_\eta^{\max} \cdot U_\eta^{\max} \quad (59)$$

$$0 \leq P_{R,GT} - P_g(t) \leq M_\eta^{\max} \cdot (1 - U_\eta^{\max}) \tag{60}$$

$$0 \leq \eta^{\min} \leq M_\eta^{\min} \cdot U_\eta^{\min} \tag{61}$$

$$0 \leq P_g(t) \leq M_\eta^{\min} \cdot (1 - U_\eta^{\min}) \tag{62}$$

$$0 \leq \gamma^{\max} \leq M_\gamma^{\max} \cdot U_\gamma^{\max} \tag{63}$$

$$0 \leq Q_{R,sto} - Q_{sto}(t) \leq M_\gamma^{\max} \cdot (1 - U_\gamma^{\max}) \tag{64}$$

$$0 \leq \gamma^{\min} \leq M_\gamma^{\min} \cdot U_\gamma^{\min} \tag{65}$$

$$0 \leq Q_{sto}(t) \leq M_\gamma^{\min} \cdot (1 - U_\gamma^{\min}) \tag{66}$$

where $U_\mu^{\max}$, $U_\mu^{\min}$, $U_\pi^{\max}$, $U_\pi^{\min}$, $U_\phi^{\max}$, $U_\phi^{\min}$, $U_\eta^{\max}$, $U_\eta^{\min}$, $U_\gamma^{\max}$, $U_\gamma^{\min}$ are 0-1 variables. $M_\mu^{\max}$, $M_\mu^{\min}$, $M_\pi^{\max}$, $M_\pi^{\min}$, $M_\phi^{\max}$, $M_\phi^{\min}$, $M_\eta^{\max}$, $M_\eta^{\min}$, $M_\gamma^{\max}$, $M_\gamma^{\min}$ are large enough constant.

According to the strong duality theory, the objective of the primal problem is equal to the objective of the corresponding dual problem. For the lower model (29)-(35), the objective function of the dual problem can be expressed as (67).

$$\begin{aligned}
\max F_e^D = \sum_{t=1}^{T} &(\lambda_t \cdot P_{load} + \mu^{\min} \cdot G_i^{\min} \\
&- \mu^{\max} \cdot G_i^{\max} - \phi^{\max} \cdot P_w^{\max} \\
&- \gamma^{\max} \cdot Q_{sto}^{\max} - \eta^{\max} \cdot P_{R,g} \\
&- \pi^{\max} \cdot P_{R,P2G})
\end{aligned} \tag{67}$$

From the optimality conditions in KKT conditions, at the optimal solution point of the lower model, $\nabla L = 0$.

$$\begin{aligned}
\frac{\partial L}{\partial G_i(t)} = \sum_{g=1}^{N_g} &((c_E - \lambda_t) \cdot \mu \cdot \eta_t \cdot \delta_t \\
&+ c_i + \lambda_t + \mu^{\max} - \mu^{\min}) = 0
\end{aligned} \tag{68}$$

$$\frac{\partial L}{\partial P_{P2G}(t)} = \sum_{p=1}^{N_p} (c_{P2G} - \lambda_t + (\pi^{\max} - \pi^{\min})) = 0 \tag{69}$$

$$\begin{aligned}
\frac{\partial L}{\partial P_w(t)} = \sum_{w=1}^{N_w} &(\lambda_t \cdot \omega_t + c_w \cdot (1 - \omega_t) \\
&+ (\phi^{\max} - \phi^{\min})) = 0
\end{aligned} \tag{70}$$

$$\frac{\partial L}{\partial P_g(t)} = \sum_{m=1}^{N_m} (\lambda_t + (\eta^{\max} - \eta^{\min}) + c_g) = 0 \tag{71}$$

$$\frac{\partial L}{\partial Q_{sto}(t)} = \sum_{t=1}^{T} (\lambda_c + (\gamma^{\max} - \gamma^{\min})) = 0 \tag{72}$$

Then (67) and (23) are substituted into the upper model, and the transformed single-level model can be obtained as (73).

$$\begin{aligned}
\max \quad &- \sum_{t=1}^{T} \sum_{j=1}^{N_j} (c_j \cdot S_j(t)) + \sum_{t=1}^{T} (\lambda_t \cdot P_{load} + \\
&\mu^{\min} \cdot G_i^{\min} - \mu^{\max} \cdot G_i^{\max} - \\
&\phi^{\max} \cdot P_w^{\max} - \gamma^{\max} \cdot Q_{sto}^{\max} - \\
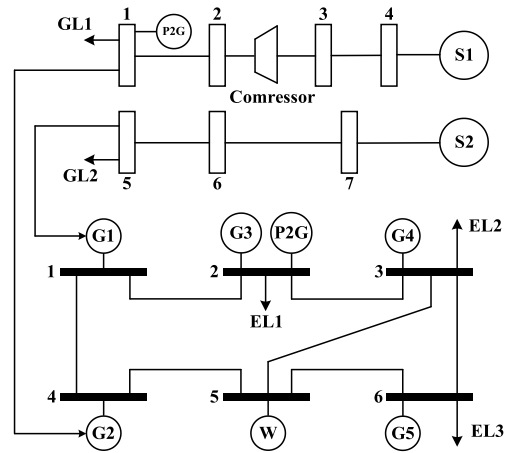&\eta^{\max} \cdot P_{R,g} - \pi^{\max} \cdot P_{R,P2G}) - F_C
\end{aligned}$$

FIGURE 7. Structure of 6-bus power system and 7-node natural gas system.

$$\begin{aligned}
s.t. \quad &(7) - (13), (18) - (20), (27) - (28), \\
&(47) - (66), (68) - (72)
\end{aligned} \tag{73}$$

V. CASE STUDIES

In this paper, a 6-bus power system/7-node natural gas system is employed as shown in Fig. 7. IEGS model with CCUS is constructed. In the power system, G1-G2 are gas turbines, G3-G5 represent CCPP, with the original carbon emissions coefficient $\delta_t = 1.1$ t/MWh, and the CO_2 capture energy consumption coefficient $\mu = 0.23$ MWh/t [32]. One end of the P2G is connected to node 2 of the electrical system and the other end is connected to node 1 of the natural gas system, the rated power of P2G is 60 MW, and the operating cost coefficient is 20 $/MW, and the conversion efficiency is 0.64. A wind farm with an installed capacity of 300 MW is connected to node 5. The electric load is evenly distributed at nodes 2, 3 and 6. The carbon trading market price is taken as 40 $/t. The gas purchase cost coefficients of the two gas sources S1 and S2 are 10.5 $/kcf and 13.5 $/kcf respectively. The time-of-use electricity prices are shown in Table 1. The electricity load, gas load, and wind power forecast are shown in Fig. 8.

A. INFLUENCE OF CCUS SYSTEM ON SCHEDULING RESULTS

The following two cases are set for comparative analysis to investigate the influence of CCUS on the operation of the integrated energy system.

Case 1: System operation and economic dispatch of IES without CCUS.

Case 2: System operation and economic dispatch of IES with CCUS.

The power distribution of each unit and the carbon emissions of the system under the two cases are shown in Fig. 9-Fig. 10. The comparison of scheduling results in the two scenarios is shown in Table 2.

CCUS includes carbon capture, utilization and storage, which can participate in system operation as a load and
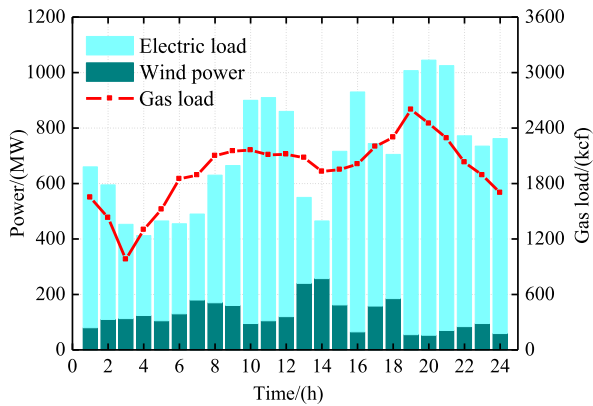
FIGURE 8. Electricity load, gas load, and wind power forecast.

TABLE 1. Time-of-use electricity price.

Time period	Price: $/MWh
0:00–8:00, 22:00–24:00	105.06
8:00–12:00, 18:00–22:00	130.36
12:00–18:00	177.24

improve the coupling between the power system and the natural gas system. SNG generated by the P2G device can be involved in the dispatch of the natural gas system and reduce the cost of gas purchase. As can be seen from Fig. 9 and Fig. 10, the thermal unit output of case 2 is higher because of the addition of power-using equipment such as P2G and carbon capture device, to achieve electrical power balance. By comparing the two cases in Table 2, it can be found that after the introduction of CCUS, since the CO_2 generated by the system operation can be captured and stored, compared with case 1, the carbon emissions and carbon transaction costs of case 2 are reduced by 3350 t and 237000 $, i.e. 51.9% and 71.8%, respectively. Because there is no P2G unit, no SNG is produced in case 1. The overall comprehensive cost of the system of case 1 is 16.1% higher than that of case 2. This shows the effectiveness of CCUS in reducing system costs and carbon emissions.

B. COMPARISON OF BI-LEVEL MODEL AND SINGLE-LEVEL MODEL

In order to further prove the rationality and effectiveness of the proposed model, the proposed bi-level and single-level models are compared. The objective function of the single-level optimization model is the sum of the upper and lower objective functions, and the constraint conditions are composed of the upper and lower model constraints. The single-level model is as (58).

$$\min \{(13) + (16)\}$$
$$s.t. \quad (7) - (13), (18) - (19), (21), (27) - (28),$$
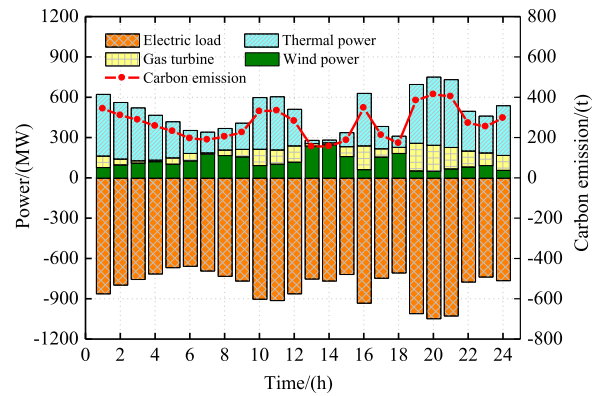$$(30) - (35) \tag{74}$$

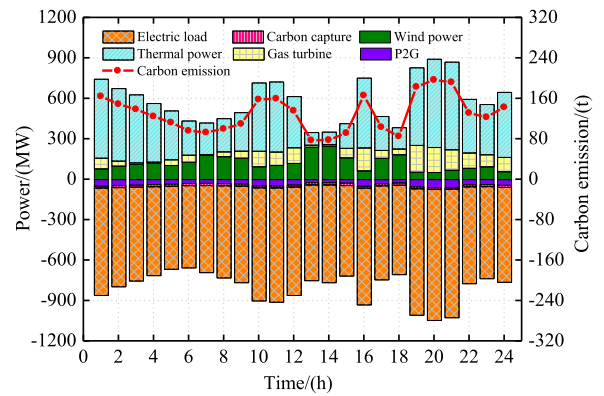**FIGURE 9.** Power distribution of case 1.

FIGURE 10. Power distribution of case 2.

Gas supply from each gas source under two models is shown in Fig. 11, the carbon emissions and SNG production of the two models are shown in Fig. 12, and the scheduling results of the two models are shown in Table 3. From Fig. 11, it can be seen that the gas supply of gas source 1 (S1) under the bi-level model is 5527 kcf more than that of the single-level model, and the gas supply of gas source 2 (S2) under the bi-level model is 5782 kcf less than that of the single-level model. This is because the gas purchase cost coefficient of S1 is lower than that of S2, and the economics of the natural gas system can be considered independently under the bi-level model, which can better respond to the natural gas price and make S1 supply more gas, so the cost of the natural gas system under the bi-level model is lower than that of the single-level model.

The objective function is the main difference between the bi-level and single-level models. The cost of the natural gas and electrical systems in the bi-level model are considered separately in the objective function. In contrast, the single-level model is a direct sum of the two systems. Because of the significant difference in the magnitude of the cost of the two systems, the single-level model cannot consider the economics of the two energy networks. The P2G unit under the bi-level model can produce more SNG, which will consume more CO_2

and reduce system carbon emissions. As can be seen from Fig. 12 and Table 3, compared with the single-level model,

TABLE 2. Comparison of dispatch results under two cases.

Case	Upper model cost/(10^5 $)	Lower model cost/(10^5 $)	Carbon trading cost/(10^5 $)	Total cost/(10^5 $)	Synthetic natural gas/(10^3 kcf)	Carbon emission/(10^3 t)
1	7.79	94.11	3.30	105.20	0	6.45
2	7.52	79.80	0.93	88.25	1.21	3.10

TABLE 3. Comparison results of two models.

Model	Natural gas system cost/(10^5 $)	Power system cost/(10^5 $)	Carbon trading cost/(10^5 $)	Total cost/(10^5 $)	Synthetic natural gas/(10^3 kcf)	Carbon emission/(10^3 t)
Single-level	7.79	87.69	1.07	96.55	1.06	3.32
Bi-level	7.52	79.80	0.93	88.25	1.21	3.10

TABLE 4. Comparison of two carbon trading mechanisms.

Carbon trading mechanism	Upper model cost/(10^5 $)	Lower model cost/(10^5 $)	Carbon trading cost/(10^5 $)	Total cost/(10^5 $)	Carbon emission/(10^3 t)
Traditional	7.76	79.02	1.08	87.86	3.32
Ladder	7.52	79.80	0.93	88.25	3.10

FIGURE 11. Gas supply from each gas source under two models.

FIGURE 12. Comparison of carbon emissions and synthetic natural gas under two models.
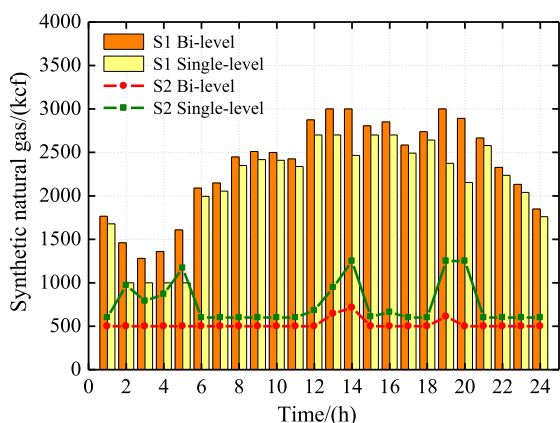
under the bi-level model, the natural gas system cost is reduced by 27000 $, the power system cost is reduced by 789000 $, carbon trading cost is reduced by 14000 $, the total system cost is is decreased by 830000 $, i.e. 8.59%, the carbon emission is decreased by 220 t, i.e. 6.63%, and the
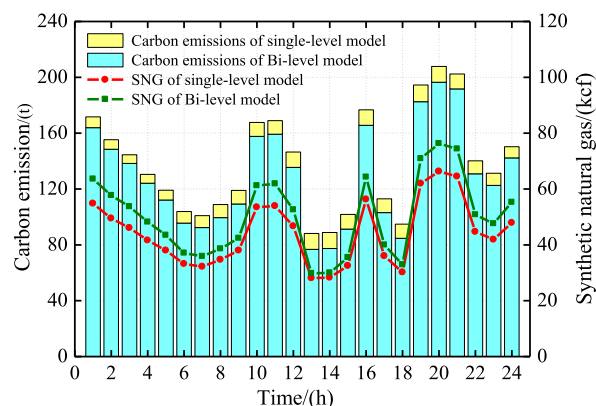
SNG is increased by 150 kcf, i.e. 12.39%. It demonstrates the bi-level optimization model is more conducive to reducing the operation cost and carbon emissions of IEGS, and more SNG are synthesized through the P2G process, which effectively
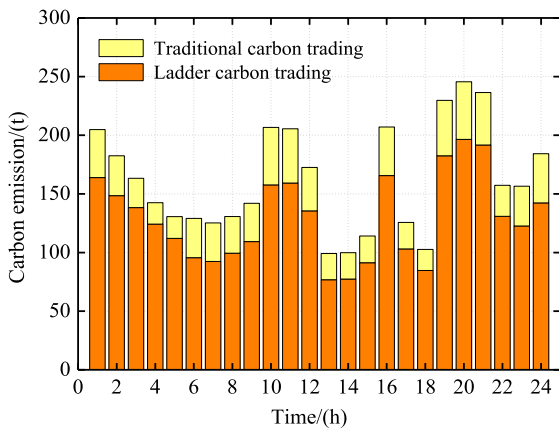
FIGURE 13. Carbon emissions under two carbon trading mechanisms.

reduces the quantity of natural gas purchased from the gas network.

C. COMPARISON OF TWO CARBON TRADING MECHANISMS

In order to verify the effectiveness of the ladder carbon trading mechanism in reducing system carbon emissions and carbon trading costs, the system scheduling results under the ladder carbon trading mechanism and the traditional carbon trading mechanism are compared. The unit carbon trading price is $c = 40$ $, carbon trading price growth rate for each tier is $s = 8$ $, carbon emission range length $x = 600$ t, carbon emission quota is $Q_t = 1200$ t. System carbon emissions under the two carbon trading mechanisms are shown in Fig. 13, and the system scheduling results are shown in Table 4.

As can be seen from Fig. 13 and Table 4, compared to the traditional carbon trading mechanism, although the total system cost under the ladder carbon trading mechanism increases by 39000 $, i.e. 0.44%, the system carbon emission decreases by 790 t, i.e. 20.3%. It proves the effectiveness of the ladder carbon trading mechanism in low-carbon economic dispatch.

VI. CONCLUSION

In this paper, a bi-level optimal scheduling model of low-carbon economic dispatch was presented for IEGS considering carbon capture, utilization and storage. The following conclusions have been drawn:

1) Compared with the single-level model that directly adds objective functions of the two systems, the bi-level model proposed in this paper reduces the system operating cost and carbon emissions, which is economical and reasonable.

2) CCUS can participate in system operation as a load and improve the coupling of power system and natural gas system operation.

3) The introduction of the ladder carbon trading mechanism divides carbon credits into multiple bands. Each band corresponds to a different carbon trading price.

Companies can purchase or sell carbon credits according to their actual requirements. It effectively raises the awareness of energy-saving and emission reduction among enterprises, which makes carbon emissions a substantial economic benefit.

In future work, we plan to consider the complementary characteristics of wind power and photovoltaic, introducing more energy into the functional side.

REFERENCES

[1] A. Akbari-Dibavar, B. Mohammadi-Ivatloo, K. Zare, T. Khalili, and A. Bidram, "Economic-emission dispatch problem in power systems with carbon capture power plants," *IEEE Trans. Ind. Appl.*, vol. 57, no. 4, pp. 3341–3351, Jul. 2021.

[2] M. F. Tahir, C. Haoyong, K. Mehmood, N. Ali, and J. A. Bhutto, "Integrated energy system modeling of China for 2020 by incorporating demand response, heat pump and thermal storage," *IEEE Access*, vol. 7, pp. 40095–40108, 2019.

[3] Y. Wang, Y. Wang, Y. Huang, J. Yang, Y. Ma, H. Yu, M. Zeng, F. Zhang, and Y. Zhang, "Operation optimization of regional integrated energy system based on the modeling of electricity-thermal-natural gas network," *Appl. Energy*, vol. 251, Oct. 2019, Art. no. 113410.

[4] R. Zhang, T. Jiang, G. Q. Li, H. H. Chen, X. Li, and R. X. Ning, "Bi-level optimization dispatch of integrated electricity-natural gas systems considering P2G for wind power accommodation," *Proc. CSEE*, vol. 38, no. 19, pp. 5668–5678, Oct. 2018.

[5] X. Guo, S. Lou, Y. Wu, and Y. Wang, "Low-carbon operation of combined heat and power integrated plants based on solar-assisted carbon capture," *J. Mod. Power Syst. Clean Energy*, vol. 10, no. 5, pp. 1138–1151, 2022.

[6] D. Song, W. Meng, M. Dong, J. Yang, J. Wang, X. Chen, and L. Huang, "A critical survey of integrated energy system: Summaries, methodologies and analysis," *Energy Convers. Manage.*, vol. 266, Aug. 2022, Art. no. 115863.

[7] A. Mazza, E. Bompard, and G. Chicco, "Applications of power to gas technologies in emerging electrical systems," *Renew. Sustain. Energy Rev.*, vol. 92, pp. 794–806, Sep. 2018.

[8] Y. Yang, Z. Luo, X. Yuan, X. Lv, H. Liu, Y. Zhen, J. Yang, and J. Wang, "Bi-level multi-objective optimal design of integrated energy system under low-carbon background," *IEEE Access*, vol. 9, pp. 53401–53407, 2021.

[9] G. Fambri, C. Diaz-Londono, A. Mazza, M. Badami, and R. Weiss, "Power-to-gas in gas and electricity distribution systems: A comparison of different modeling approaches," *J. Energy Storage*, vol. 55, Nov. 2022, Art. no. 105454.

[10] J. T. Chen, P. Yang, and Y. Chen, "Optimal operation of park multi-energy systems based on comprehensive demand-side response strategies," *Renew. Energy*, vol. 39, no. 2, pp. 222–228, Nov. 2021.

[11] X. Fang, Q. Hu, F. Li, B. Wang, and Y. Li, "Coupon-based demand response considering wind power uncertainty: A strategic bidding model for load serving entities," *IEEE Trans. Power Syst.*, vol. 31, no. 2, pp. 1025–1037, Mar. 2016.

[12] X. Tian, X. Lin, W. Zhong, and Y. Zhou, "Security assessment of electricity-gas-heat integrated energy systems based on the vulnerability index," *Energy*, vol. 249, Jun. 2022, Art. no. 123673.

[13] Z. Wei, S. Zhang, G. Sun, X. Xu, and S. Chen, "Carbon trading based low-carbon economic operation for integrated electricity and natural gas energy system," *Autom. Electr. Power Syst.*, vol. 40, no. 15, pp. 9–16, Aug. 2016.

[14] G. Yuan, Y. Gao, and B. Ye, "Optimal dispatching strategy and real-time pricing for multi-regional integrated energy systems based on demand response," *Renew. Energy*, vol. 179, pp. 1424–1446, Dec. 2021.

[15] X. Chen and X. Wu, "The roles of carbon capture, utilization and storage in the transition to a low-carbon energy system using a stochastic optimal scheduling approach," *J. Cleaner Prod.*, vol. 366, Sep. 2022, Art. no. 132860.

[16] S. Zhou, K. Sun, Z. Wu, W. Gu, G. Wu, Z. Li, and J. Li, "Optimized operation method of small and medium-sized integrated energy system for P2G equipment under strong uncertainty," *Energy*, vol. 199, May 2020, Art. no. 117269.

[17] S. Qiu, J. Chen, C. Mao, Q. Duan, C. Ma, Z. Liu, and D. Wang, "Day-ahead optimal scheduling of power–gas–heating integrated energy system considering energy routing," *Energy Rep.*, vol. 8, pp. 1113–1122, Nov. 2022.

[18] B. Miao, J. Lin, H. Li, C. Liu, B. Li, X. Zhu, and J. Yang, "Day-ahead energy trading strategy of regional integrated energy system considering energy cascade utilization," *IEEE Access*, vol. 8, pp. 138021–138035, 2020.

[19] J. R. Guo, Y. Xiang, and J. J. Wu, "Low-carbon optimal scheduling of electricity-gas integrated energy systems considering CCUS-P2G technology and risk of carbon market," *Proc. CSEE*, vol. 43, no. 4, pp. 1290–1303, Feb. 2023.

[20] D. Yang, Y. Xu, X. Liu, C. Jiang, F. Nie, and Z. Ran, "Economic-emission dispatch problem in integrated electricity and heat system considering multi-energy demand response and carbon capture technologies," *Energy*, vol. 253, Aug. 2022, Art. no. 124153.

[21] L. He, Z. Lu, J. Zhang, L. Geng, H. Zhao, and X. Li, "Low-carbon economic dispatch for electricity and natural gas systems considering carbon capture systems and power-to-gas," *Appl. Energy*, vol. 224, pp. 357–370, Aug. 2018.

[22] E. Korani and A. Eydi, "Bi-level programming model and KKT penalty function solution approach for reliable hub location problem," *Expert Syst. Appl.*, vol. 184, Dec. 2021, Art. no. 115505.

[23] R. Guo, H. Ye, and Y. Zhao, "Low carbon dispatch of electricity-gas-thermal-storage integrated energy system based on stepped carbon trading," *Energy Rep.*, vol. 8, pp. 449–455, Nov. 2022.

[24] X. Li, T. Li, L. Liu, Z. Wang, X. Li, J. Huang, J. Huang, P. Guo, and W. Xiong, "Operation optimization for integrated energy system based on hybrid CSP-CHP considering power-to-gas technology and carbon capture system," *J. Cleaner Prod.*, vol. 391, Mar. 2023, Art. no. 136119.

[25] Z. Zhang, C. Wang, H. Lv, F. Liu, H. Sheng, and M. Yang, "Day-ahead optimal dispatch for integrated energy system considering power-to-gas and dynamic pipeline networks," *IEEE Trans. Ind. Appl.*, vol. 57, no. 4, pp. 3317–3328, Jul. 2021.

[26] T. M. Alabi, L. Lu, and Z. Yang, "Data-driven optimal scheduling of multi-energy system virtual power plant (MEVPP) incorporating carbon capture system (CCS), electric vehicle flexibility, and clean energy marketer (CEM) strategy," *Appl. Energy*, vol. 314, May 2022, Art. no. 118997.

[27] C. He, L. Wu, T. Liu, and M. Shahidehpour, "Robust co-optimization scheduling of electricity and natural gas systems via ADMM," *IEEE Trans. Sustain. Energy*, vol. 8, no. 2, pp. 658–670, Apr. 2017.

[28] Z. Ji, C. Kang, Q. Chen, Q. Xia, C. Jiang, Z. Chen, and J. Xin, "Low-carbon power system dispatch incorporating carbon capture power plants," *IEEE Trans. Power Syst.*, vol. 28, no. 4, pp. 4615–4623, Nov. 2013.

[29] S. Luo, C. Chen, W. Qiu, J. Ma, L. Yang, and Z. Lin, "Bi-layer optimal planning of rural distribution network based on KKT condition and big-M method," *Energy Rep.*, vol. 7, pp. 637–644, Nov. 2021.

[30] C. Wang, W. Wei, J. Wang, F. Liu, and S. Mei, "Strategic offering and equilibrium in coupled gas and electricity markets," *IEEE Trans. Power Syst.*, vol. 33, no. 1, pp. 290–306, Jan. 2018.

[31] Y. Xiang, G. Wu, X. Shen, Y. Ma, J. Gou, W. Xu, and J. Liu, "Low-carbon economic dispatch of electricity-gas systems," *Energy*, vol. 226, Jul. 2021, Art. no. 120267.

[32] P. Luo, W. L. Yan, and Y. Wang, "Robust optimal scheduling of integrated electricity-gas-heat energy systems considering CCUS," *High Voltage Eng.*, vol. 48, no. 6, pp. 2077–2087, Aug. 2022.

XINGHUA LIU (Senior Member, IEEE) received the B.Sc. degree from Jilin University, Changchun, China, in 2009, and the Ph.D. degree in automation from the University of Science and Technology of China, Hefei, China, in 2014.

From 2014 to 2015, he was invited as a Visiting Fellow with RMIT University, Melbourne, VIC, Australia. From 2015 to 2018, he was a Research Fellow with the School of Electrical and Electronic Engineering, Nanyang Technological University, Singapore. He has been a Professor with the Xi'an University of Technology, Xi'an, China, since 2018. His current research interests include integrated energy systems, intelligent systems, cyber-physical systems, robotic systems, state estimation and control, and autonomous vehicles.

XIANG LI (Student Member, IEEE) received the B.S. degree in electrical engineering from the Xi'an University of Technology, Xi'an, China, in July 2020, where he is currently pursuing the M.S. degree. His research interests include the economic dispatch of integrated energy systems and low-carbon technology.

JIAQIANG TIAN received the B.S. degree in automation from Xi'an Technological University, Xi'an, China, in 2016, and the Ph.D. degree in control science and engineering from the University of Science and Technology of China, Hefei, China, in 2021.

From July 2021 to December 2022, he worked as a Lecturer at the School of Electrical Engineering, Xi'an University of Technology. Since January 2023, he has been working with the School of Electrical Engineering and Automation, Anhui University. His research interests include energy storage modeling, fault diagnosis, energy management, and optimal scheduling of integrated energy systems.

GUOQING YANG received the B.S. and M.S. degrees from the Xi'an University of Technology and the Ph.D. degree from Xi'an Jiaotong University. He is currently a professor and a supervisor of master's students. His main research interests include gas discharge mechanisms and applications, nano-insulation materials, and smart grids.

HUIBAO WU received the degree in power generation and power system automation from Xi'an Electric Power College. He has been working with State Grid Xi'an Electric Power Supply Company, since 1998. His research interest includes power system operation and management.

RONG HA received the B.S. degree in computer information management from Xidian University. He has been working with Xi'an Jinze Electric Technology Company Ltd., since 2014. His research interests include system integration and reliability design.

PENG WANG (Fellow, IEEE) received the B.Sc. degree in electrical engineering from Xi'an Jiaotong University, Xi'an, China, in 1978, the M.Sc. degree in electrical engineering from the Taiyuan University of Technology, Taiyuan, China, in 1987, and the M.Sc. and Ph.D. degrees in electrical engineering from the University of Saskatchewan, Saskatoon, SK, Canada, in 1995 and 1998, respectively.

He is currently a Professor with Nanyang Technological University, Singapore. His research interests include power system planning and operation, renewable energy planning, solar/electricity conversion systems, and power system reliability analysis. He served as an Associate Editor for IEEE TRANSACTIONS ON SMART GRID and a Guest Editor for *Journal of Modern Power Systems and Clean Energy*'s special issues on smart grids. He also served as an Associate Editor for IEEE TRANSACTIONS ON POWER DELIVERY and as the Guest Editor-in-Chief for *CSEE Journal of Power and Energy Systems*'s special issues on hybrid AC/DC grids for future power systems.

● ● ●